Supplementary Information

Structural basis of cargo recognition by the myosin-X MyTH4-FERM domain

Yoshinori Hirano, Taiki Hatano, Aya Takahashi, Michinori Toriyama, Naoyuki Inagaki and Toshio Hakoshima

Nara Institute of Science and Technology, Japan

Supplementary figures

Supplementary Figure S1

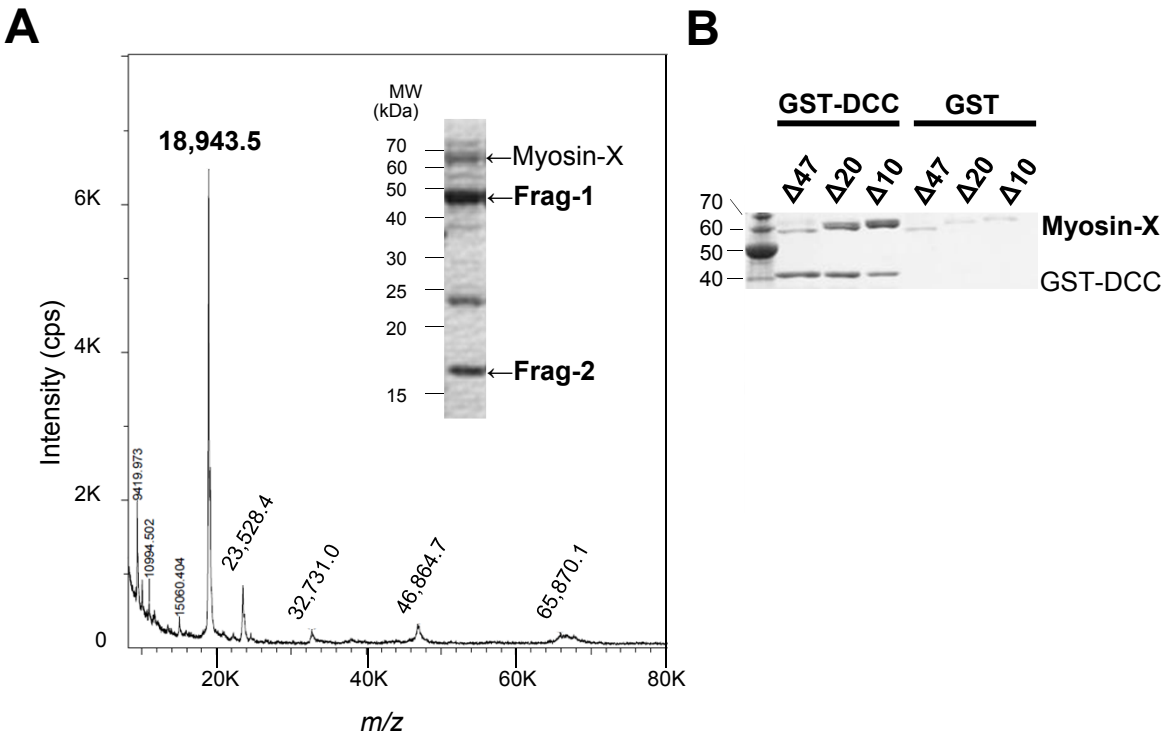

Figure S1 Identification of the degradation loop of the human myosin-X MyTH4-FERM cassette.

(**A**) A TOF-MS spectrum of the fragment-1 (Frag-1) from the protein sample of the myosin-X MyTH4-FERM cassette. The inset shows the SDS-PAGE pattern of the sample. The protein sample of the recombinant human MyTH4-FERM cassette produces two major fragments (Frag-1 and Frag-2) during purification. A TOF-MS spectrum of Frag-2 showed a major peak corresponding to a molecular mass of 18,943.5 Da, which is closely related to the calculated value of 18,966 for a fragment of myosin-X residues Phe1893-Arg2058. The N-terminal analysis of Frag-2 suggested the N-terminal sequence of FRTGSV (data not shown), which is consistent with the proposed fragment. The peak at a *m/Z* value of 65,870.1 may correspond to trace amounts of the full-length protein of the construct and the peak at 46,864.7 to Frag-1. The observed *m/Z* value and our N-terminal analysis indicate that Frag-1 corresponds to residues 1486-1888 plus two extra residues (Gly-Pro) that were part of the HRV3C protease-recognition sequence (calculated 46,855 Da). Since Frag-2 corresponds to residues 1893-2058, only 4 residues are missing from our fragments.

(**B**) Binding assay of deletion mutants of the myosin-X MyTH4-FERM cassette. The deletion mutants *Δ*47 (residues1845-1891), *Δ*20 (1872-1891) and *Δ*10 (1882-1891) are served for pull-down assays with GST-fused DCC P3 peptide (GST-DCC).

Supplementary Figure S2

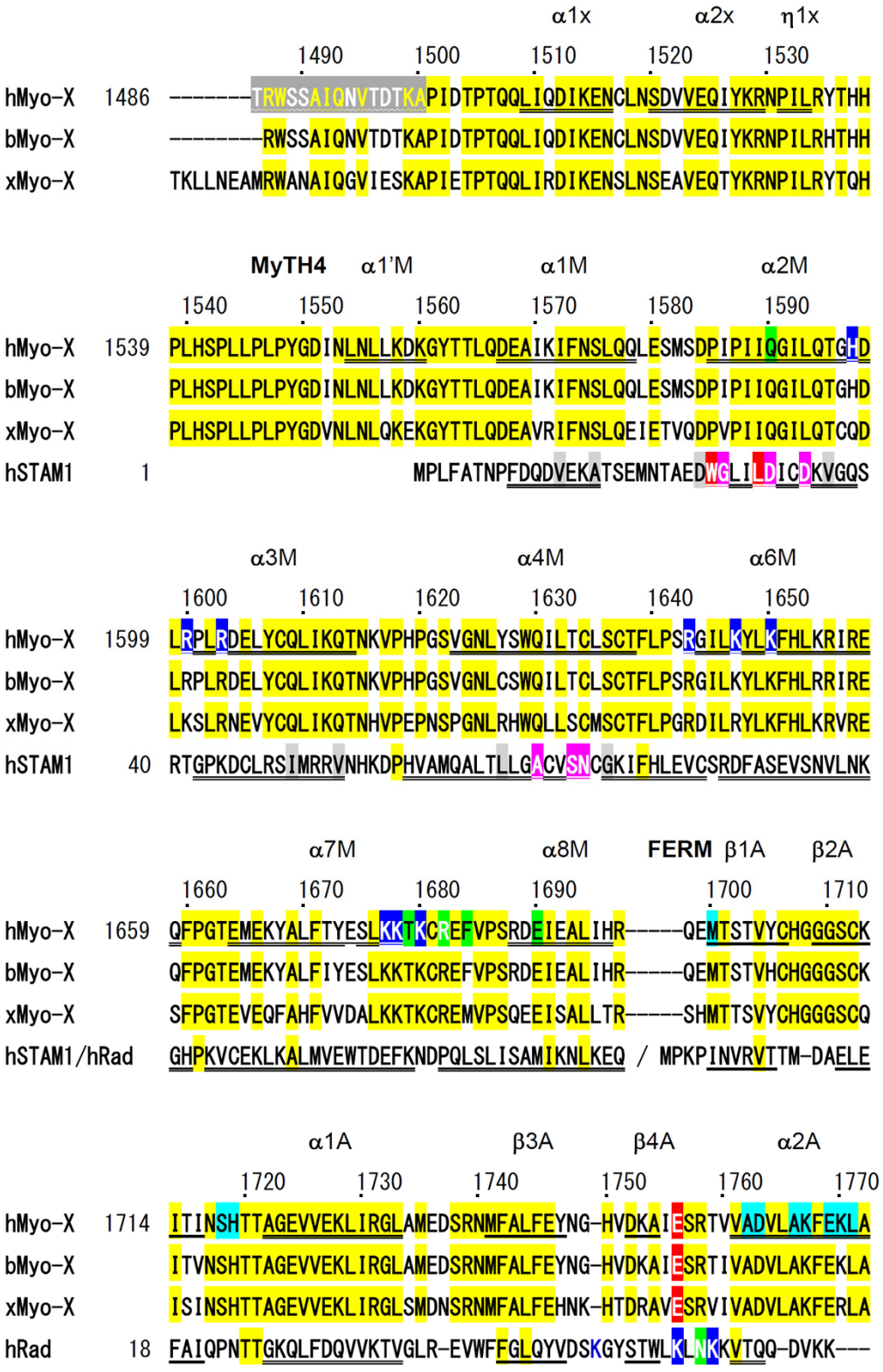

Supplementary Figure S2 (continued)

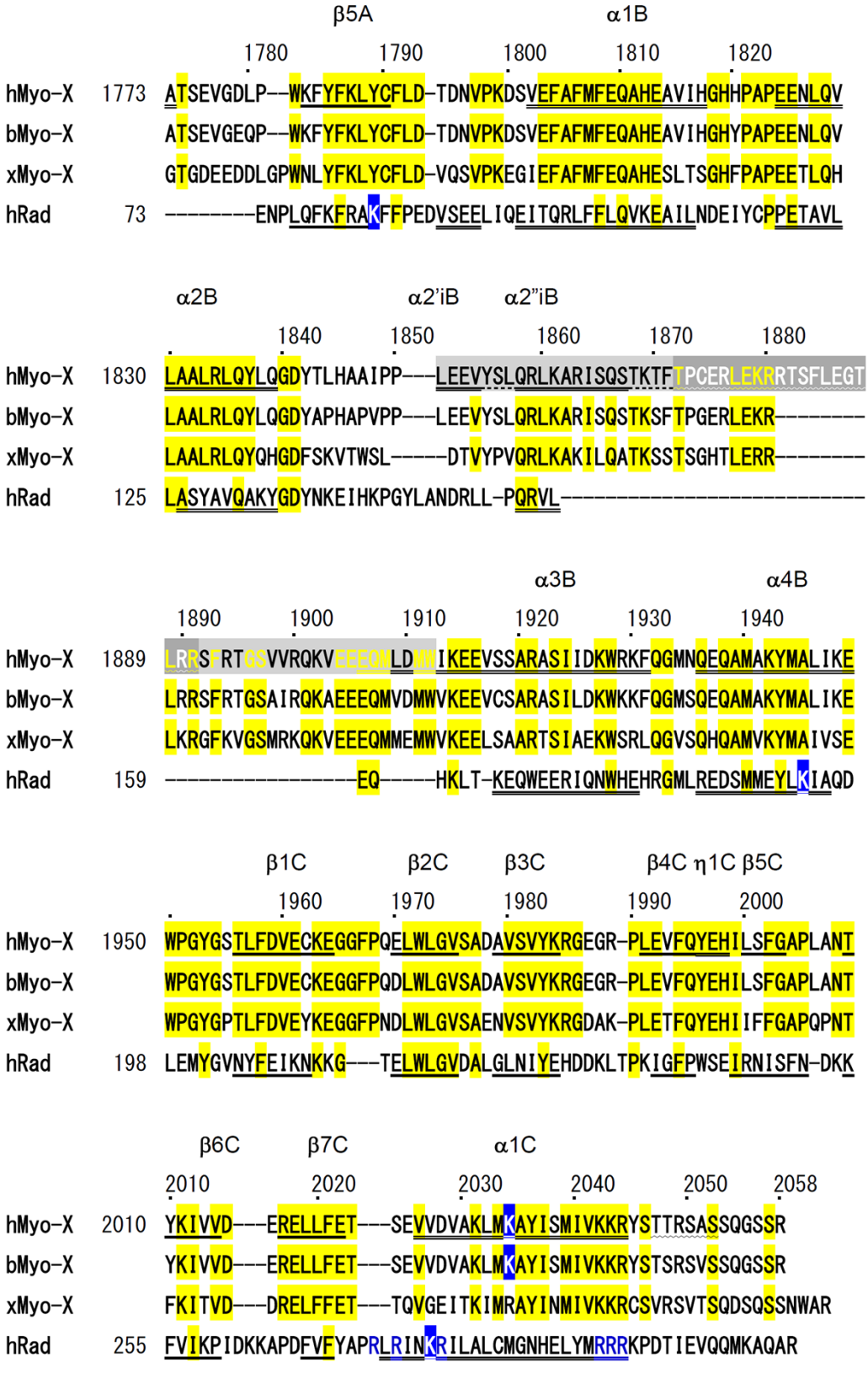

Supplementary Figure S2 (continued)

Figure S2 Sequence alignment and secondary structures of the myosin-X MyTH4-FERM cassette.

Human, bovine and xenopus MyTH4-FERM cassettes are aligned with conserved residues highlighted in yellow (hMyo-X, bMyo-X and xMyo-X, respectively). Secondary structures are indicated with double underlines (α-helices) and single bold underlines (β-strands). In the current map of hMyo-X, N-terminal residues (1486-1500), which include T1486 and R1487 believed to belong to the upstream PH2 domain, and 12 C-terminal residues (2047-2058) were not defined. These residues are highlighted in grey with white letters and wavy underlines. Compared with radixin, the insertion residues (1851-1891) of human myosin-X are highlighted in grey, with deleted residues (1872-1891) shown as white letters. Basic residues that form the basic patch on the MyTH4 domain of human myosin-X are highlighted in blue. Residues that participate in forming the interface between the MyTH4 and FERM domains are highlighted in green and cyan, respectively.

The MyTH4 domain is also aligned with the VHS domain of human STAM1 (hSTAM1), and the FERM domain is aligned with the human radixin FERM domain (hRad). In the crystal structure of the STAM1 VHS domain bound to ubiquitin (PDB ID 3LDZ), key residues that directly interact with ubiquitin are highlighted in red (critical) or pink (not essential), with other residues (grey) conserved in the VHS domains. In the crystal structure of the radixin FERM domain bound to IP_3 (PDB ID 1GC6), key residues that directly interact with IP_3 are highlighted in blue or green, and other basic residues that participate in the basic cleft between subdomains A and C are shown as blue letters.

Supplementary Figure S3

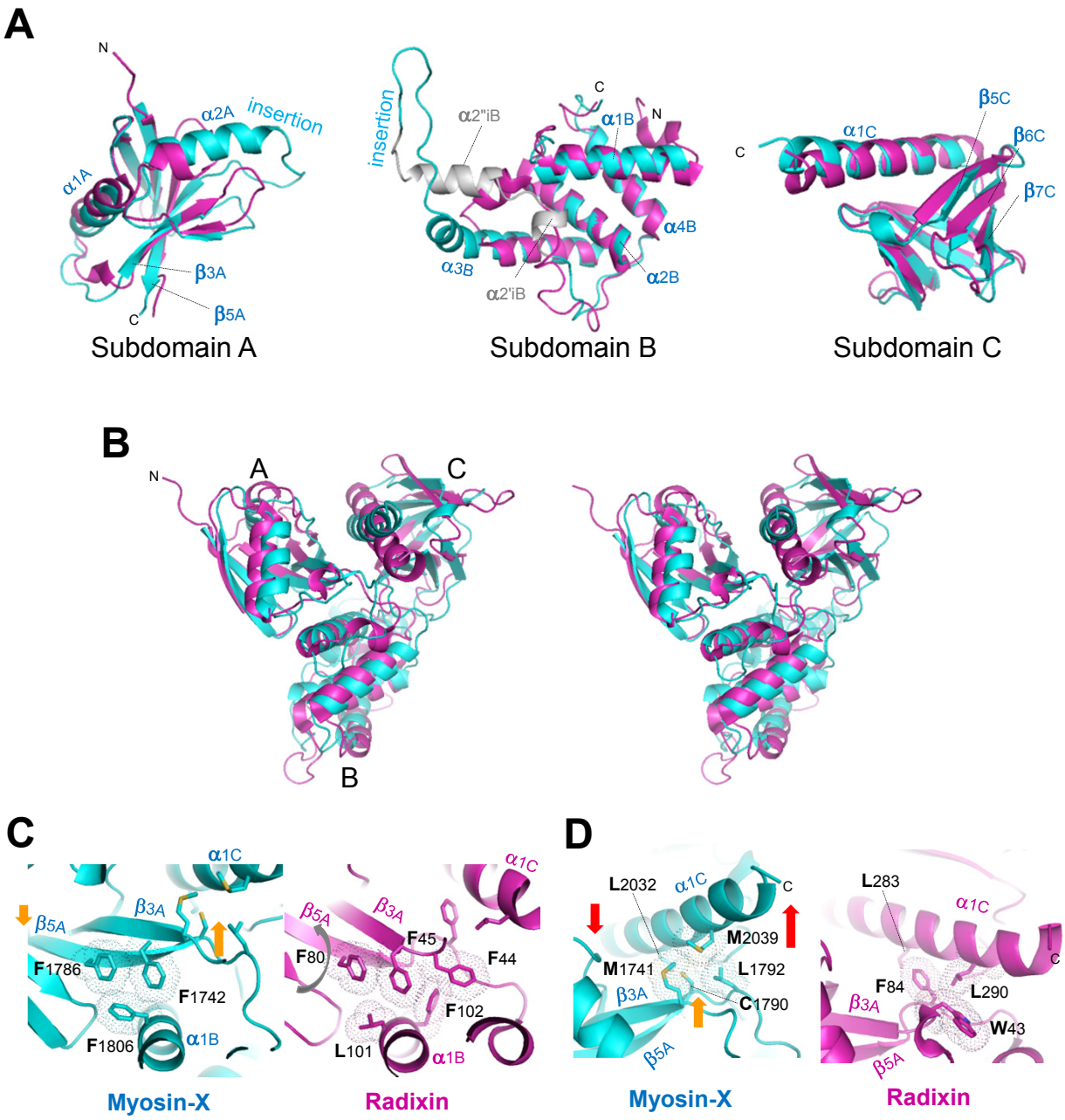

Supplementary Figure S3 (continued)

Figure S3 Comparison between FERM domains of myosin-X and radixin.

(**A**) Individual superposition of subdomains A, B and C from the myosin-X (cyan) and radixin (magenta) FERM domains with r.m.s. deviations of 2.3 Å (75 residues, 13% identity), 2.1 Å (102 residues, 22% identity) and 1.4 Å (86 residues, 20% identity), respectively. The poorly conserved extra residues of subdomains A and B are indicated with a label “insertion”.

(**B**) Stereo-view of superimposition of FERM domains of myosin-X (cyan) and radixin (magenta) with a relatively large r.m.s. deviation of 4.8 Å for 273 residues that exhibit 18% identity.

(**C**) A shift in subdomain A orientation and position relative to subdomain B is induced by contacts made by the β5A and β3A strands from subdomain A with the α1B helix from subdomain B. In the myosin-X FERM domain (*left*, cyan), subdomain A has a longer β-sheet comprising the β3A (Phe1742) and β5A (Phe1786) strands that sits on the α1B helix (Phe1806) of subdomain B, pushing one side of the β-sheet contacting the α1C helix upward from subdomain B. Contacts involving aromatic rings are shown. In the radixin FERM domain (*right*, magenta), subdomain A has a shorter β-sheet comprising the β3A (Phe45) and β5A (Phe80) strands. This sheet and the flanking α1A-β3A loop (Phe44) make contact with the α1B helix (Leu101 and Phe102) of subdomain B.

(**D**) A large shift in subdomain C orientation and position relative to subdomain B is induced by contacts involving the linker between subdomains A and B. In the myosin-X FERM domain (*left*, cyan), the β5A-α1B loop (Leu1792), and the β5A (Cys1790) and β3A (Met1741) strands push the C-terminal end of the α1C helix (Met2039) upwards. In the radixin FERM domain (*right*, magenta), Phe84 (β5A-α1B loop) and Trp43 (α1A-β3A loop) make contact with Leu290 (α1C). The rotation of subdomain C is pivoted on myosin-X Leu2032 (α1C), which corresponds to radixin Leu283 (α1C).

Supplementary Figure S4

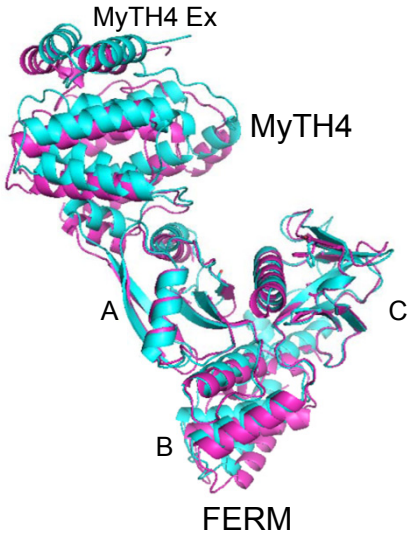

Figure S4 Structural comparison of the myosin-X MyTH4-FERM domain cassettes obtained in this study.

The crystal of the free form of the myosin-X MyTH4-FERM domain cassettes contain two crystallographically independent molecules. Two molecules A (magenta) and B (grey) of the free forms are superimposed on the DCC-bound form (cyan).

Supplementary Figure S5

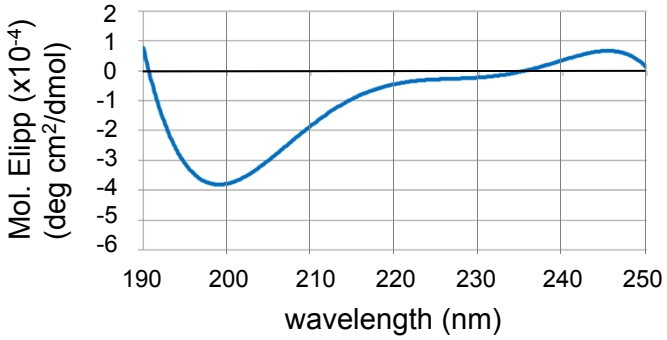

Figure S5 CD spectrum of the DCC P3 peptide (1373-1477).

The spectrum obtained clearly suggested the absence of typical secondary structures such as the α-helix at a sample concentration of ~0.1 mg/ml (13 μM). CD spectra were recorded using a JASCO J-720W spectropolarimeter at 20°C. Secondary structure estimations were calculated using the JASCO Secondary Structure Estimation software.

Supplementary Figure S6

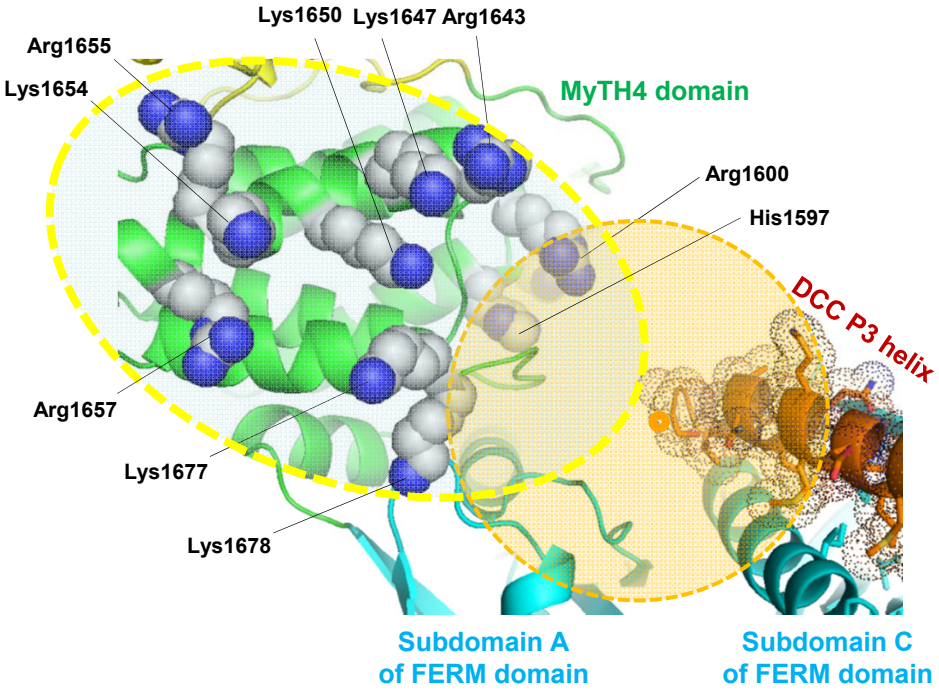

Figure S6 Basic residues of the MyTH4 domain and the FERM-bound DCC P3 helix.

The C-terminus of the DCC P3 helix has a peptide stretch (Gly-Ser-Ala-Phe-COOH) which is flexible in our crystal, probably due to the glycine residue, and the last two residues are absent in our structure. These residues occupy the space (orange gradation) with a radius of about 10 Å or 15 Å and could reach some basic residues of the MyTH4 domain. Thus, the C-terminal flexible peptide region could interfere with accommodation of the tubulin C-terminal acidic tail at the concave region formed by MyTH4 and FERM domains.

Supplementary Figure S7

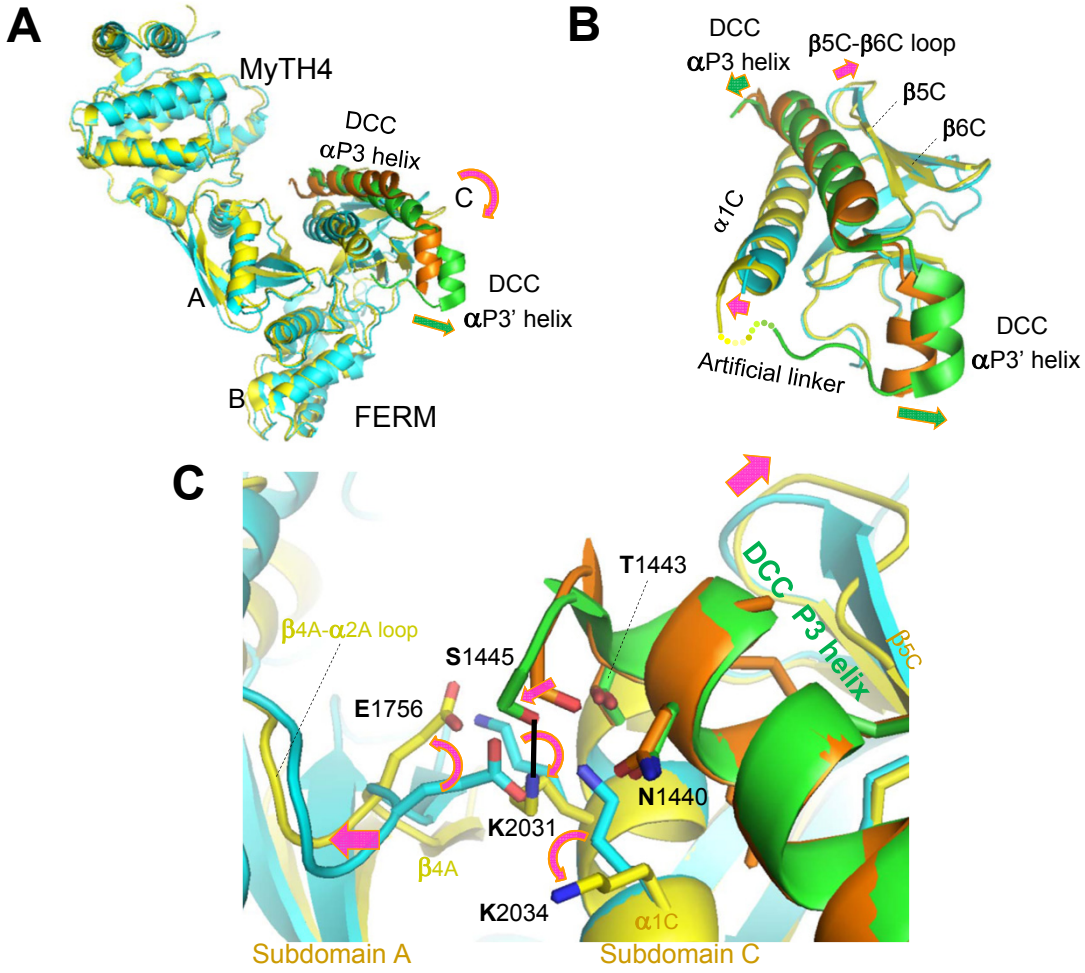

Figure S7 Structural comparison of our myosin-X MyTH4-FERM-DCC complex with the MyTH4-FERM-DCC fusion protein.

(A) Superimposition of the myosin-X MTH4-FERM cassettes of our complex (cyan) and the recently-reported fused protein (PDB ID 3PZD, yellow) with an r.m.s. deviation of 1.9 Å for 494 residues. The DCC peptide (orange) of our complex is shown with the fused DCC peptide (green) of the fusion protein. The observed reorientation of subdomain C is indicated by a pink arrow and a shift of the bound DCC peptide by a green arrow.

(B) Superimposition of subdomain C's of our complex (cyan) and the fusion protein (yellow) with an r.m.s. deviation of 0.8 Å for 89 residues.

(C) A close-up view of the fused DCC peptide (green) bound to subdomain C of the fusion protein (yellow) superimposed upon our complex (cyan) and the bound DCC peptide (orange). The hydrogen bond between Lys2031 and Ser1445 of the fusion protein is shown with a black solid line.

Supplementary Figure S8

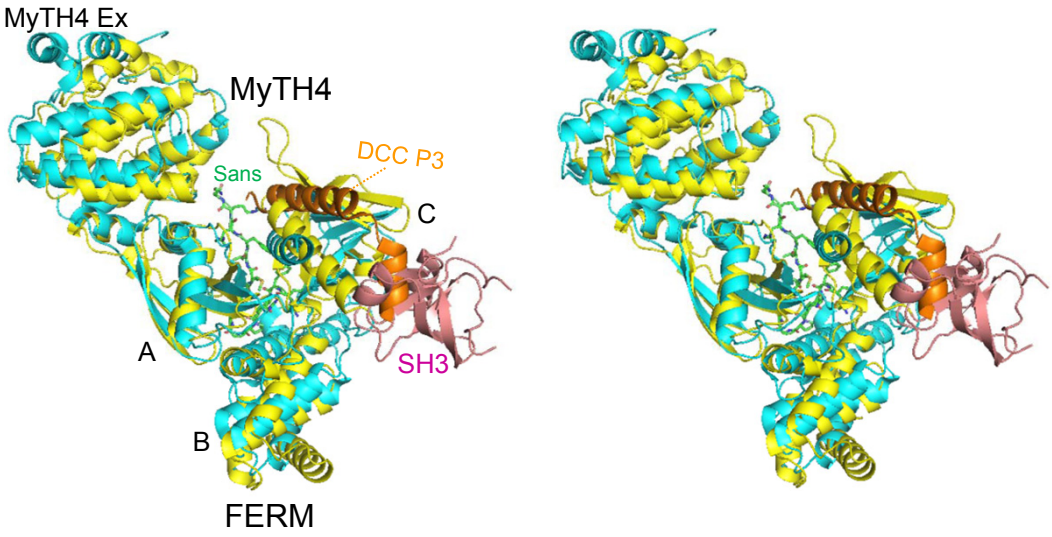

Figure S8 Structural comparison of our myosin-X MyTH4-FERM - DCC complex with the myosin-VIIa MyTH4-FERM-SH3 - Sans complex.

Stereo-view of superimposition of MTH4-FERM cassettes of myosin-X (cyan) and myosin-VIIa (PDB ID 3PVL, yellow) with an r.m.s. deviation of 6.2 Å for 432 residues. The myosin-X MyTH4-FERM cassette binds DCC P3 peptide (orange) and the myosin-VIIa MyTH4- FERM cassette is linked to the SH3 domain (pink) and binds Sans CEN peptide (a green stick model).